Biochemical and Biophysical Research Communications 421 (2012) 403–407

Contents lists available at SciVerse ScienceDirect

Biochemical and Biophysical Research Communications

journal homepage: www.elsevier.com/locate/ybbrc

Crystal structure of receiver domain of putative NarL family response regulator spr1814 from *Streptococcus pneumoniae* in the absence and presence of the phosphoryl analog beryllofluoride

Ae Kyung Park [a,1], Jin Ho Moon [b,1], Ki Seog Lee [c], Young Min Chi [a,*]

[a] Division of Biotechnology, College of Life Sciences, Korea University, Seoul 136-713, Republic of Korea
[b] Insititute of Life Sciences and Natural Resources, Korea University, Seoul 136-713, Republic of Korea
[c] Department of Clinical Laboratory Science, College of Health Sciences, Catholic University of Pusan, Busan 609-757, Republic of Korea

ARTICLE INFO

Article history:
Received 5 April 2012
Available online 10 April 2012

Keywords:
Two-component phosphotransfer pathways
Response regulator
Receiver domain
Phosphoryl analog beryllofluoride

ABSTRACT

Spr1814 of *Streptococcus pneumoniae* is a putative response regulator (RR) that has four-helix helix-turn-helix DNA-binding domain and belongs to the NarL family. The prototypical RR contains two domains, an N-terminal receiver domain linked to a variable effector domain. The receiver domain functions as a phosphorylation-activated switch and contains the typical doubly wound five-stranded α/β fold. Here, we report the crystal structure of the receiver domain of spr1814 (spr1814$_R$) determined in the absence and presence of beryllofluoride as a phosphoryl analog. Based on the overall structure, spr1814$_R$ was shown to contain the typical fold similar with other structures of the receiver domain; however, an additional linker region connecting the receiver and DNA-binding domain was inserted into the dimer interface of spr1814$_R$, resulting in the formation of unique dimer interface. Upon phosphorylation, the conformational change of the linker region was observed and this suggests that domain rearrangement between the receiver domain and effector domain could occur in full-length spr1814.

1. Introduction

Bacteria sense and respond to a wide variety of signals through a complex network of signaling systems, many of which are two-component phosphotransfer pathways. These systems regulate many processes, including nutrient uptake, sporulation, chemotaxis, virulence, quorum sensing, and cell adhesion [1]. In the simplest form, a two-component system consists of two modular proteins, a sensory histidine kinase (HK) and a response regulator (RR) [2]. The HK phosphorylates at a specific His residue by itself, then the phosphoryl group is transferred to a conserved Asp residue in the N-terminal regulatory domain of the RR. The phosphorylation event induces the activation of the C-terminal effector domain of the RR, which binds to specific DNA sequences in most two-component systems, and regulates transcriptional initiation [3]. The transcription factor RRs are further divided into subfamilies, including the OmpR/PhoB winged-helix domain [4,5], the NarL/FixJ four-helix helix-turn-helix domain [6,7], the NtrC/DctD AAA + ATPase domain fused to a factor of inversion (Fis)-type helix-turn-helix domain [8], and the recently characterized LytTR domain, which contains an unusual, predominantly β fold [9]. In diverse RRs, different types of conformational change are found to occur upon phosphorylation. Phosphorylation can promote the dimerization (StyR [10] and PhoB [11]), and induce a higher oligomerization state (NtrC [12]). Moreover, it has been suggested that the NarL/FixJ family is activated by phosphorylation-induced domain rearrangements disrupting the inter-domain contacts [13,14].

The spr1814 from *Streptococcus pneumoniae* belongs to the NarL/FixJ family based on similarities of the effector domains, and it has been predicted to regulate the neighboring ABC transporter, which regulates antibiotic transport with its cognate histidine kinase. The structures of receiver domains have been solved for several RRs and the structures exhibit a doubly wound five-stranded α/β fold. The conserved Asp residue located in the C-terminal edge of the β3 strand is the phosphorylation site of the receiver domain and the phosphoryl group is stabilized by the divalent cation, Mg^{2+}.

In this report, we present the crystal structures of the receiver domain of response regulator spr1814 from *Streptococcus pneumoniae* (spr1814$_R$) complexed with and without the phosphoryl analog beryllofluoride (BeF_3^-) at a resolution of 2.2 and 1.9 Å, respectively. Although the structure of spr1814$_R$ had a similar overall fold with other receiver domain structures, there was a unique additional linker region (residues 121–130) connecting the receiver and effector domains. The comparison between

* Corresponding author. Fax: +82 2 921 3702.
E-mail address: ezeg@korea.ac.kr (Y.M. Chi).
[1] These authors equally contributed.

0006-291X/$ - see front matter © 2012 Elsevier Inc. All rights reserved.
http://dx.doi.org/10.1016/j.bbrc.2012.04.035

Table 1
Data collection and refinement statistics.

	Native	BeF_3^- complex
Data collection		
Space group	$P2_1$	$P2_12_12_1$
Cell dimension (Å)	a = 52.87, b = 44.95, c = 59.3, β = 98.98°	a = 75.84, b = 83.98, c = 49.51
Resolution range (Å)	50–2.2 (2.20–2.24)	50–1.9 (1.90–1.97)
Total reflections	68.349	248.110
Unique reflections	13.021	25.704
Redundancy	5.2 (3.0)	9.7 (5.9)
Completeness (%)	91.6 (64.6)	99.6 (98.4)
[a] R_{merge} (%)	4.0 (12.3)	8.4 (32.5)
<I/σ(I)>	47.5 (6.9)	19.0 (2.5)
Refinement		
[b] R/R_{free} (%)	21.4/27.3	18.6/22.6
RMS deviation of		
Bond length (Å)	0.009	0.008
Bond angle (°)	1.2	1.1
No. of atoms		
Protein/waters	261/33	262/274
In Ramachandran plot		
Most favored (%)	95.3	97.3
Additionally allowed (%)	3.9	1.9

Values in parentheses are for the highest resolution shells.
[a] $R_{merge} = \sum_{hkli}|I_{hkli} - \langle I_{hkl}\rangle|/\sum_{hkli} I_{hkli}$, where I represents the observed intensity,$\langle I\rangle$ represents the average intensity, and i counts through all symmetry-related reflections.
[b] $R = \sum||F_{obs}| - |F_{calc}||/\sum|F_{obs}|$, where R_{free} is calculated for a randomly chosen 5% of reflections, which were not used for structure refinement.

inactivated and activated states of $spr1814_R$ shows the structural perturbations at the dimer interface, including linker region, and this result indirectly indicates that rearrangement between two domains could be triggered to activate the effector domain of spr1814.

2. Materials and methods

2.1. Cloning, overexpression and purification

Residues 1–130 of spr1814 were cloned from *S. pneumoniae* genomic DNA by the polymerase chain reaction (PCR) and inserted into the NdeI/XhoI-digested expression vector, pET28a vector (Novagen). The expression construct introduced a hexa-histidine tag at the N-terminus. The constructed plasmid was transformed into *Escherichia coli* strain BL21 (DE3) cells for expression. Transformed cells were cultured in Luria–Bertani (LB) medium containing 50 μg ml^{-1} kanamycin at 37 °C. Protein expression was induced by the addition of 0.5 mM isopropyl-β-D-1-thiogalactopyranoside (IPTG) once the cells had reached an optical density at 600 nm of about 0.45. The cells were then grown for an additional 12 h at 18 °C and harvested. Cells were resuspended in buffer A (20 mM Tris–HCl, pH 7.9, 500 mM NaCl, 5 mM imidazole) and lysed by sonication. Lysate was centrifuged for 45 min at 20,000*g*. the soluble fraction was loaded onto a Ni^{2+}-charged chelated HiTrap chelating HP column (GE Healthcare) equilibrated with buffer A. The protein was eluted with a linear gradient of buffer A containing 1 M imidazole. The protein was purified to its final state by gel filtration on a HiLoad 16/60 Superdex 200 column (GE Healthcare,) that had previously been equilibrated with buffer B (20 mM Tris–HCl, pH 7.9, 200 mM NaCl, 5 mM $MgCl_2$, 10% glycerol). The protein was finally concentrated using an Amicon Ultra-15 ultrafiltration device (Millipore) to 10 mg ml^{-1}. The protein concentration was determined using a Bradford assay.

2.2. Crystallization, data collection and structure determination

$Spr1814_R$ was subjected to screening for crystal growth using the sitting-drop vapor-diffusion method (0.5 μl protein solution and 0.5 μl reservoir solution equilibrated against 50 μl reservoir solution). All crystallization trials were performed at 22 °C. Crystals were obtained in buffers consisting of 0.1 M Tris–HCl, pH 8.0 and 28% PEG 4000. Crystal growth was scaled up using the hanging-drop vapor-diffusion method in 24-well VDX plates (Hampton Research, USA). Each hanging drop was prepared by mixing 1 μl protein solution and 1 μl reservoir solution and equilibrated over a 500 μl reservoir solution. For cocrystallization with BeF_3^- the protein solution was mixed with 30 mM NaF and 5 mM $BeCl_2$. The BeF_3^- complex crystals were obtained under the same conditions that produced native crystals.

X-ray diffraction data were collected on beamline 6C at the Pohang Light Source (Pohang, South Korea). Both crystals were cryo-protected by the introduction of 20% (v/v) ethylene glycol, and frozen in liquid nitrogen for data collection. X-ray diffraction data were collected to a resolution of 2.2 Å from native crystals and 1.9 Å from BeF_3^- complex crystals. All data sets were indexed, processed and scaled using the HKL-2000 software package [15].

The crystal structure was solved by the molecular-replacement method using the *MOLREP* program in the *CCP4* package [16] with the putative DNA binding response regulator of *Staphylcoccus aureus* (PDB ID: 3B2N) [17] as a search model. The space group of native structure was a monoclinic $P2_1$ and the space group of $BeFk_3^-$ complex structure was $P2_12_12_1$. The refinement was performed by *phenix.refine* [18] and the model was rebuilt with the *Coot* [19]. The final model of the native structure contained one dimer and two Mg^{2+} ions and the final R_{cryst} and R_{free} values were 21.4% and 27.3%, respectively. The final model of the BeF_3^- complex structure also contained one dimer, two Mg^{2+} ions, and two BeF_3^- and the final R_{cryst} and R_{free} values were 18.6% and 22.6%, respectively. The stereochemical quality of all the final models as assessed by *PROCHECK* [20] was excellent. The data-collection and final refinement statistics are given in Table 1.

2.3. Protein data bank accession number

The atomic coordinates and structure factors of native and BeF_3^- complex structure have been deposited in the Protein Data Bank, http://www.rcsb.org/pdb (PDB ID codes: 4E7O and 4E7P).

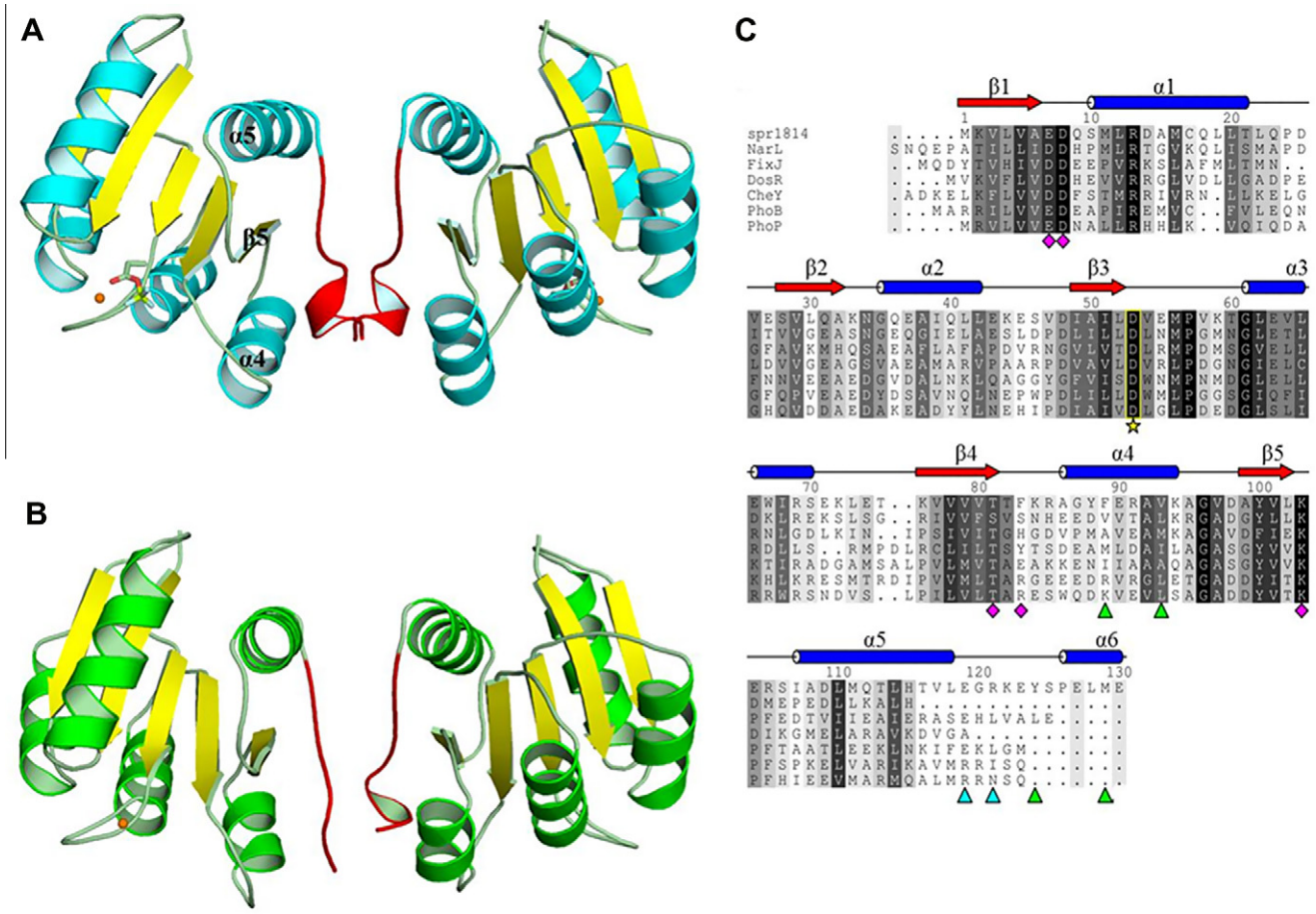

Fig. 1. (a) The overall structure of spr1814$_R$ in the activated state. The bound Mg^{2+} ions and phosphoryl analog beryllofluoride (BeF_3^-) are presented using a sphere and stick model, respectively. The α helices and β strands are colored as cyan and yellow, respectively. The linker region (residue 121–130) connecting the receiver and DNA-binding domains, is highlighted in red. (b) The overall structure of spr1814$_R$ in the inactivated state. The bound Mg^{2+} ions are shown as spheres. The α helices and β strands are colored as green and yellow, respectively. The linker region is highlighted in red. (c) Sequence alignment of the receiver domains. Completely conserved residues are shown in black boxes with white characters. Secondary structure elements of spr1814$_R$ from *S. pneumoniae* are labeled above the sequence. Residues that participate in phosphorylation are indicated by magenta diamonds. The green triangles and cyan triangles indicate the residues that participate in the dimer interface through hydrophobic interaction and salt bridges, respectively. The conserved aspartic acid residue is indicated by yellow star. NarL, PDB ID: 1RNL; FixJ, PDB ID: 1D5W; DosR, PDB ID: 3C3W; CheY, PDB ID: 1FQW; PhoB, PDB ID: 1ZES; PhoP, 2DL1. (For interpretation of the references to colour in this figure legend, the reader is referred to the web version of this article.)

3. Results and discussion

3.1. Overall structures

The crystal structure of the receiver domain of spr1814 (spr1814$_R$) was determined in the absence and presence of the phosphoryl analog beryllofluoride (BeF_3^-) at resolutions of 2.2 and 1.9 Å, respectively. The spr1814$_R$ structure was shown to contain the typical α/β fold and a $(\beta\alpha)_5$ arrangement was observed in other RRs, which had been built by five parallel β strands assembled in a central β sheet with the β2β1β3β4β5 topology, where the sheet was surrounded by five α helices (α2, α3, and α4 on one side, and α1 and α5 on the other). There were two molecules in the asymmetric unit of the activated and inactivated state forming a dimer (Fig. 1a and b). The Mg^{2+} ion was observed in both the inactivated and activated state. The amino acid sequence of the spr1814$_R$ is shown in Fig. 1c, along with locations of α helices and β strands observed in this crystal structure analysis. Although spr1814$_R$ shares low sequence similarity with response regulators, which were structurally identified in previous reports, the residues corresponding to phosphorylation site were well conserved.

In the predicted secondary structure of spr1814, a linker region connecting the receiver and DNA-binding domains was observed and was predicted to contain 20 residues, including one alpha helix. In the structure of spr1814$_R$, the part of the linker region (residues Gly121–Glu130) was observed in both the inactivated and activated states (Fig. 1a and b). This region contained a unique structure that was not observed in other the receiver domain structures. The linker region was inserted into the α4-β5-α5 interface and contributed to dimerization. Upon phosphorylation, remarkable conformational changes in the dimerization surface, which was composed of an α4-β5-α5 interface and the linker region, were observed.

3.2. Dimer interface

A majority of the dimerization interfaces characterized to date within the receiver domain were in the α4-β5-α4 region. The inactivated and activated states of spr1814$_R$ formed a dimer in the same manner using the same α4-β5-α5 interface. In many RR response regulators, such as FixJ [21], Spo0A [22], and most of the OmpR/PhoB subfamily RRs from *E. coli*, phosphorylation mediates dimerization of the receiver domains, which is thought to promote DNA binding and transcription activation. Therefore, the dimer formation of the inactivated state of spr1814$_R$ may be the

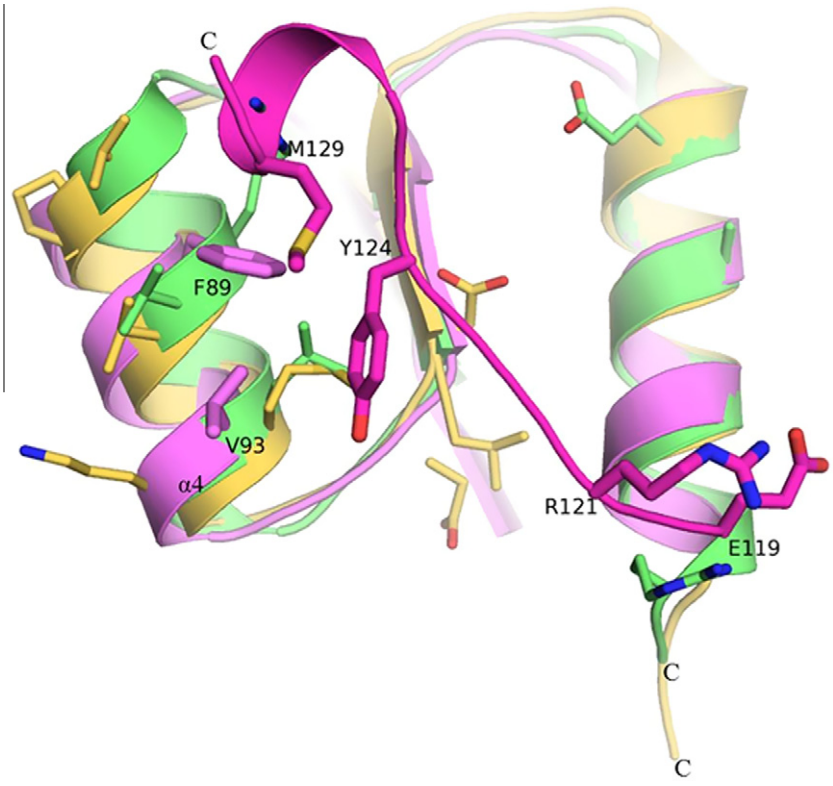

Fig. 2. Superposition of the dimer interfaces from active spr1814R (light pink) with active the receiver domains of FixJ (light orange) and PhoB (lime). The linker region of spr1814$_R$ is highlighted by magenta, and the residues that participate in the dimer interactions are presented as a stick model. (For interpretation of the references to colour in this figure legend, the reader is referred to the web version of this article.)

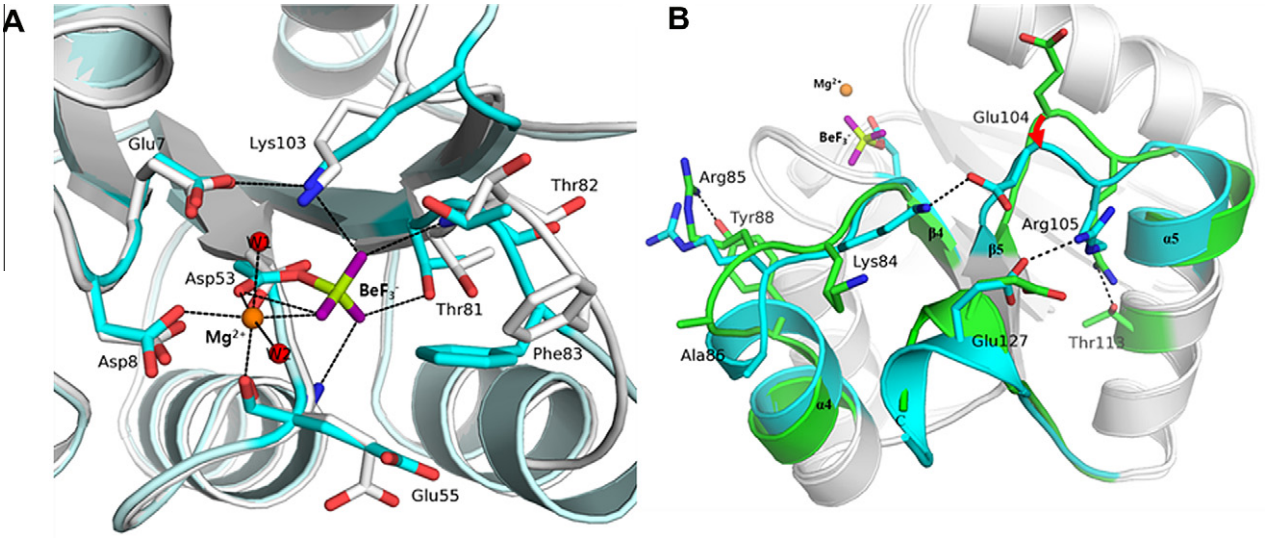

Fig. 3. (a) Close-up view of the phosphorylation site. The activated and inactivated states of spr1814$_R$ are colored as white and cyan, respectively. The residues that participate in the phosphorylation are shown as stick model. The bound Mg^{2+} ions and phosphoryl analog beryllofluoride (BeF_3^-) are presented as a sphere and stick model, respectively. (b) Comparison of the dimer interface between the inactive and active state of spr1814$_R$. The structures of inactive and active states of spr1814$_R$ are colored as green and cyan, respectively. The Glu104 which shows the remarkable conformational change is highlighted by red arrow. (For interpretation of the references to colour in this figure legend, the reader is referred to the web version of this article.)

result of the high protein concentrations, which was similar to the receiver domain of PhoP [23].

In the receiver domain structure of FixJ, the dimer interface was provided by the helix α4 and strand β5 from each receiver domain. The dimer interface was formed through mainly hydrophobic interactions by Val87, Pro88, Ala90, Val91, Met94, and Val99, and there was only one salt bridge between Lsy95 and Asp100 [14]. In the receiver domain structure of PhoP, Val88, Leu91, and Ala110 also comprised the hydrophobic patch and six residues (Lsy87-Glu107, Asp96-Arg118, and Asp97-Arg111) participated in salt bridges [23]. In the same manner, the dimer interface of spr1814$_R$ was also formed by hydrophobic interactions. The protein–protein interface involved van der Waals interactions, which were provided by the side chains of Phe89, Val93, Tyr124, and Met129, and only polar interaction that was due to the formation of salt bridges between Glu119 in one protomer and Arg121 in

the second protomer. Although, spr1814$_R$ dimerizes using the α4-β5-α5 interface, it had a unique feature when compared with the other structures. A part of the linker region, including the α6 helix, was inserted into the dimer interface, therefore this linker region also contributed to dimerization (Fig. 2). In contrast to the other structures, where the residues participating in the dimer interface resided in the α4-β5-α5 face, for spr1814$_R$, all residues, except Phe89 and Val93, which were locate in the α4 helix, were located in the linker region. In spr1814$_R$, the linker region plays an important role in the dimer interaction, which was not observed in other reported structures.

3.3. Conformational changes upon phosphorylation

The active site of spr1814$_R$, in addition to the site of phosphorylation, an Asp53 in the loop following β3, contained two additional Glu7 and Asp8 residues that coordinated an essential Mg^{2+} ion, and a conserved Lys103 residue that formed a salt bridge with the phosphate in the activated domain. The conformations of the conserved active-site residues in the active form of spr1814$_R$ were similar to those of equivalent residues in other activated receiver domain. The density of the Mg^{2+} and BeF_3^- complex noncovalently bound to Asp53 is clearly seen in the electron density map of the BeF_3^- complex structure, and binding of the BeF_3^- induced no significant conformational changes in the conserved residues (Fig. 3a). The Mg^{2+} was coordinated with the fluoride atom 1 (F1) from BeF_3^- the side chain carboxyl oxygens of Asp8 and Asp53, and the main chain carbonyl oxygen of Glu55. The two water molecules were liganded to the metal ion, which displayed perfect octahedral coordination. The conserved Lys103 was found to be involved in salt bridges with Glu7 and F3 of BeF_3^- Upon phosphorylation, the conserved Thr81, which was located at the C-terminal end of β4, was in an inward orientation and formed a hydrogen bond with the F2 of BeF_3^- which was oriented away from the active pocket in the inactivated state. The rotation of Thr81 was accompanied by a rotation of the backbone N of the next residue Thr82, which formed a hydrogen bond with F3. Then, Phe83 filled the cavity left by the Thr81 reorientation. The conformational changes of the two conserved switch residues (Thr81 and Phe83) upon phosphorylation at the active site induced structural perturbations at the distal α4-β4-α5 surface, which mediated the dimer interface.

When the root-mean-square deviations (RMSD) between the activated and inactivated state of spr1814$_R$ was calculated, the highest RMSD values was achieved in the two loop regions (β4-α4 and β5-α5, specifically Arg85 and Glu104), which formed the dimer interface and showed the largest structural perturbations upon phosphorylation at other receiver domains (Fig. 3b). In the inactivated state, NH1 of Arg85 was found to be hydrogen bonded with OH of Tyr88 and NH2 of Arg105 was hydrogen bonded with OG1 of Thr113. Upon phosphorylation, the above two interactions disappeared, whereas two salt-bridges were generated. The Glu104 showed a remarkable conformational change and the interactions between Glu104–Lys84 and Arg105–Glu127 were main forces driving the structural perturbations upon phosphorylation. Among them, the interaction between Arg105 and Glu127 was determined to be a unique feature in regards to the interaction with the receiver domain and linker region. The comparison between inactivated and activated structures showed that phosphorylation induced structural perturbations at the dimer interface, including the linker region, which can cause domain rearrangement.

Acknowledgments

We thank the staff at beamline 6C of Pohang Light Source, South Korea, for assistance during the data collection. This work was supported by a Korea Research Foundation Grant (KRF-2007-359-C00026) funded by the Korean Government (MOEHRD).

References

[1] A.M. Stock, V.L. Robinson, P.N. Goudreau, Two-component signal transduction, Annu. Rev. Biochem. 69 (2000) 183–215.
[2] J.S. Parkinson, E.C. Kofoid, Communication modules in bacterial signaling proteins, Annu. Rev. Genet. 26 (1992) 71–112.
[3] R. Gao, A.M. Stock, Biological insights from structures of two-component proteins, Annu. Rev. Microbiol. 63 (2009) 133–154.
[4] E. Martinez-Hackert, A.M. Stock, Structural relationships in the OmpR family of winged-helix transcription factors, J. Mol. Biol. 269 (1997) 301–312.
[5] M. Solá, F.X. Gomis-Rüth, L. Serrano, A. Gonzálelz, M. Coll, Three-dimensional crystal structure of the transcription factor PhoB receiver domain, J. Mol. Biol. 285 (1999) 675–687.
[6] I. Baikalov, I. Schröder, M. Kaczor-Grzeskowiak, K. Grzeskowiak, R.P. Gunsalus, R.E. Dickerson, Structure of the *Escherichia coli* response regulator NarL, Biochemistry 35 (1996). 11503-11061.
[7] M. Milani, L. Leoni, G. Rampioni, E. Zennaro, P. Ascenzi, M. Bolognesi, An active-like structure in the unphosphorylated StyR response regulator suggests a phosphorylation-dependent allosteric activation mechanism, Structure 13 (2005) 1289–1297.
[8] J.D. Batchelor, M. Doucleff, C.J. Lee, K. Matsubara, S. De Carlo, J. Heideker, M.H. Lamers, J.G. Pelton, D.E. Wemmer, Structure and regulatory mechanism of *Aquifex aeolicus* NtrC4: variability and evolution in bacterial transcriptional regulation, J. Mol. Biol. 384 (2008) 1058–1075.
[9] D.J. Sidote, C.M. Barbieri, T. Wu, A.M. Stock, Structure of the *Staphylococcus aureus* AgrA LytTR domain bound to DNA reveals a beta fold with an unusual mode of binding, Structure 16 (2008) 727–735.
[10] L. Leoni, P. Ascenzi, A. Bocedi, G. Rampioni, L. Castellini, E. Zennaro, Styrene-catabolism regulation in *Pseudomonas fluorescens* ST: phosphorylation of StyR induces dimerization and cooperative DNA-binding, Biochem. Biophys. Res. Commun. 303 (2003) 926–931.
[11] P. Bachhawat, G.V. Swapna, G.T. Montelione, A.M. Stock, Mechanism of activation for transcription factor PhoB suggested by different modes of dimerization in the inactive and active states, Structure 13 (2005) 1353–1363.
[12] C. Wyman, I. Rombel, A.K. North, C. Bustamante, S. Kustu, Unusual oligomerization required for activity of NtrC, a bacterial enhancer-binding protein, Science 275 (1997) 1658–1661.
[13] J.H. Zhang, G. Xiao, R.P. Gunsalus, W.L. Hubbell, Phosphorylation triggers domain separation in the DNA binding response regulator NarL, Biochemistry 42 (2003) 2552–2559.
[14] C. Birck, L. Mourey, P. Gouet, B. Fabry, J. Schumacher, P. Rousseau, D. Kahn, J.P. Samama, Conformational changes induced by phosphorylation of the FixJ receiver domain, Structure 7 (1999) 1505–1515.
[15] Z. Otwinowski, M. Minor, Processing of X-ray diffraction data collected in oscillation mode, Methods Enzymol. 276 (1997) 307–326.
[16] A. Vagin, A. Teplyakov, MOLREP: an automated program for molecular replacement, J. Appl. Cryst. 30 (1997) 1022–1025.
[17] PDB ID: 3B2N. V.N. Malashkevich, R. Toro, A.J. Meyer, J.M. Sauder, S.K. Burley, S.C. Almo. Crystal structure of DNA-binding response regulator, LuxR family, from *Staphylococcus aureus*.
[18] P.D. Adams, R.W. Grosse-Kunstleve, L.W. Hung, T.R. Ioerger, A.J. McCoy, N.W. Moriarty, R.J. Read, J.C. Sacchettini, N.K. Sauter, T.C. Terwilliger, PHENIX: building new software for automated crystallographic structure determination, Acta Cryst. D58 (2002) 1948–1954.
[19] P. Emsley, K. Cowtan, Coot: model-building tools for molecular graphics, Acta Crystallogr. D60 (2004) 2126–2132.
[20] R.A. Laskowski, M.V. MacArthur, D.S. Moss, J.M. Thornton, PROCHECK: a program to check the stereochemical quality of protein structures, J. Appl. Crystallogr. 26 (1993) 283–291.
[21] S. Da Re, J. Schumacher, P. Rousseau, J. Fourment, C. Ebel, D. Kahn, D, Phosphorylation-induced dimerization of the FixJ receiver domain, Mol. Microbiol. 34 (1999) 504–511.
[22] R.J. Lewis, D.J. Scott, J.A. Brannigan, J.C. Ladds, M.A. Cervin, G.B. Spiegelman, J.G. Hoggett, I. Barák, A.J. Wilkinson, Dimer formation and transcription activation in the sporulation response regulator Spo0A, J Mol Biol. 316 (2002) 235–245.
[23] P. Bachhawat, A.M. Stock, Crystal structure of the receiver domain of the response regulator PhoP from *Escherichi coli* in the absence and presence of the phosphoryl analog beryllofluoride, J. Bacteriol. 189 (2007) 5987–5995.